



Heriot-Watt University

Heriot-Watt University
Research Gateway

Mid-infrared spectral broadening in an ultrafast laser inscribed gallium lanthanum sulphide waveguide

McCarthy, John E.; Bookey, Henry T.; Psaila, Nicholas D.; Thomson, Robert R.; Kar, Ajoy Kumar

Published in:
Optics Express

DOI:
[10.1364/OE.20.001545](https://doi.org/10.1364/OE.20.001545)

Publication date:
2012

[Link to publication in Heriot-Watt Research Gateway](#)

Citation for published version (APA):

McCarthy, J. E., Bookey, H. T., Psaila, N. D., Thomson, R. R., & Kar, A. K. (2012). Mid-infrared spectral broadening in an ultrafast laser inscribed gallium lanthanum sulphide waveguide. *Optics Express*, 20(2), 1545-1551. [10.1364/OE.20.001545](https://doi.org/10.1364/OE.20.001545)



Mid-infrared spectral broadening in an ultrafast laser inscribed gallium lanthanum sulphide waveguide

John E. McCarthy,¹ Henry T. Bookey,¹ Nicholas D. Psaila,² Robert R. Thomson,¹ and Ajoy K. Kar^{1,*}

¹Scottish University Physics Alliance, Department of Physics, School of Engineering and Physical Sciences, David Brewster Building, Heriot-Watt University, Edinburgh, EH11 4AS, United Kingdom

²Optoscribe, Ltd., Alba Innovation Centre, Alba campus, Livingston, EH54 7GA, United Kingdom
*a.k.kar@hw.ac.uk

Abstract: We report the successful fabrication of mid-infrared waveguides written in a gallium lanthanum sulphide (GLS) substrate via the ultrafast laser inscription technique. Single mode guiding at 2485 nm and 3850 nm is observed. Spectral broadening spanning 1500 nm (−15dB points) is demonstrated under 3850 nm excitation.

©2012 Optical Society of America

OCIS codes: (130.4310) Nonlinear; (320.6629) Supercontinuum generation.

References and links

1. A. Kosterev, G. Wysocki, Y. Bakhrin, S. So, R. Lewicki, M. Fraser, F. Tittel, and R. F. Curl, "Application of quantum cascade lasers to trace gas analysis," *Appl. Phys. B* **90**(2), 165–176 (2008).
2. P. Lucas, M. A. Solis, D. Le Coq, C. Juncker, M. R. Riley, J. Collier, D. E. Boesewetter, C. Boussard-Plédel, and B. Bureau, "Infrared biosensors using hydrophobic chalcogenide fibers sensitized with live cells," *Sens. Actuators B Chem.* **119**(2), 355–362 (2006).
3. P. Houizot, C. Boussard-Plédel, A. J. Faber, L. K. Cheng, B. Bureau, P. A. Van Nijnatten, W. L. M. Gieleesen, J. Pereira do Carmo, and J. Lucas, "Infrared single mode chalcogenide glass fiber for space," *Opt. Express* **15**(19), 12529–12538 (2007).
4. M. Balu, J. Hales, D. J. Hagan, and E. W. Van Stryland, "Dispersion of nonlinear refraction and two-photon absorption using a white-light continuum Z-scan," *Opt. Express* **13**(10), 3594–3599 (2005).
5. R. Grille, G. Martin, L. Labadie, B. Arezki, P. Kern, T. Lewi, A. Tsun, and A. Katzir, "Single mode mid-infrared silver halide asymmetric flat waveguide obtained from crystal extrusion," *Opt. Express* **17**(15), 12516–12522 (2009).
6. L. Le Neindre, F. Smektala, K. Le Foulgoc, X. H. Zhang, and J. Lucas, "Tellurium halide optical fibers," *J. Non-Cryst. Solids* **242**(2-3), 99–103 (1998).
7. C. Tsay, Y. Zha, and C. B. Arnold, "Solution-processed chalcogenide glass for integrated single-mode mid-infrared waveguides," *Opt. Express* **18**(25), 26744–26753 (2010).
8. A. Zakery and S. R. Elliott, "Optical properties and applications of chalcogenide glasses: a review," *J. Non-Cryst. Solids* **330**(1-3), 1–12 (2003).
9. Z. G. Lian, W. J. Pan, D. Furniss, T. M. Benson, A. B. Seddon, T. Kohoutek, J. Orava, and T. Wagner, "Embossing of chalcogenide glasses: monomode rib optical waveguides in evaporated thin films," *Opt. Lett.* **34**(8), 1234–1236 (2009).
10. C. Tsay, E. Mujagić, C. K. Madsen, C. F. Gmachl, and C. B. Arnold, "Mid-infrared characterization of solution-processed As₂Se₃ chalcogenide glass waveguides," *Opt. Express* **18**(15), 15523–15530 (2010).
11. M. Frumar, B. Frumarova, P. Nemeč, T. Wagner, J. Jedelsky, and M. Hrdlicka, "Thin Chalcogenide films prepared by pulsed laser deposition – new amorphous materials applicable in optoelectronics and chemical sensors," *J. Non-Cryst. Solids* **352**(6-7), 544–561 (2006).
12. K. M. Davis, K. Miura, N. Sugimoto, and K. Hirao, "Writing waveguides in glass with a femtosecond laser," *Opt. Lett.* **21**(21), 1729–1731 (1996).
13. Y. Cheng, K. Sugioka, and K. Midorikawa, "Freestanding optical fibers fabricated in a glass chip using femtosecond laser micromachining for lab-on-a-chip application," *Opt. Express* **13**(18), 7225–7232 (2005).
14. R. R. Thomson, H. T. Bookey, N. D. Psaila, A. Fender, S. Campbell, W. N. Macpherson, J. S. Barton, D. T. Reid, and A. K. Kar, "Ultrafast-laser inscription of a three dimensional fan-out device for multicore fiber coupling applications," *Opt. Express* **15**(18), 11691–11697 (2007).

15. H. T. Bookey, R. R. Thomson, N. D. Psaila, A. K. Kar, N. Chiodo, R. Osellame, and G. Cerullo, "Femtosecond laser inscription of low insertion loss waveguides in Z-cut lithium niobate," *IEEE Photon. Technol. Lett.* **19**(12), 892–894 (2007).
16. S. M. Eaton, H. Zhang, M. L. Ng, J. Z. Li, W. J. Chen, S. Ho, and P. R. Herman, "Transition from thermal diffusion to heat accumulation in high repetition rate femtosecond laser writing of buried optical waveguides," *Opt. Express* **16**(13), 9443–9458 (2008).
17. R. R. Thomson, T. A. Birks, S. G. Leon-Saval, A. K. Kar, and J. Bland-Hawthorn, "Ultrafast laser inscription of an integrated photonic lantern," *Opt. Express* **19**(6), 5698–5705 (2011).
18. A. Martinez, M. Dubov, I. Khrushchev, and I. Bennion, "Direct writing of fibre Bragg gratings by femtosecond laser," *Electron. Lett.* **40**(19), 1170–1172 (2004).
19. N. D. Psaila, R. R. Thomson, H. T. Bookey, S. Shen, N. Chiodo, R. Osellame, G. Cerullo, A. Jha, and A. K. Kar, "Supercontinuum generation in an ultrafast laser inscribed chalcogenide glass waveguide," *Opt. Express* **15**(24), 15776–15781 (2007).
20. M. A. Hughes, W. Yang, and D. W. Hewak, "Spectral broadening in femtosecond laser written waveguides in Chalcogenide glass," *J. Opt. Soc. Am. B* **26**(7), 1370–1378 (2009).
21. M. Sheik-Bahae, A. A. Said, T. H. Wei, D. J. Hagan, and E. W. Van Stryland, "Sensitive measurement of optical nonlinearities using a single beam," *IEEE J. Quantum Electron.* **26**(4), 760–769 (1990).
22. J. T. Gopinath, M. Soljačić, E. P. Ippen, V. N. Fuflyigin, W. A. King, and M. Shurgalin, "Third order nonlinearities in Ge-As-Se- based glasses for telecommunications applications," *J. Appl. Phys.* **96**(11), 6931–6933 (2004).
23. X. Orignac, D. Barbier, X. Min Du, R. M. Almeida, O. McCarthy, and E. Yeatman, "Sol-Gel silica/titania-on-silicon Er/Yb-doped waveguides for optical amplification at 1.5 μm ," *Opt. Mater.* **12**(1), 1–18 (1999).
24. G. Genty, M. Lehtonen, H. Ludvigsen, J. Broeng, and M. Kaivola, "Spectral broadening of femtosecond pulses into continuum radiation in microstructured fibers," *Opt. Express* **10**(20), 1083–1098 (2002).
25. G. Agrawal, *Nonlinear Fiber Optics*, 3rd ed. (Academic Press, 2001).
26. D. Blömer, A. Szameit, F. Dreisow, T. Schreiber, S. Nolte, and A. Tünnermann, "Nonlinear refractive index of fs-laser-written waveguides in fused silica," *Opt. Express* **14**(6), 2151–2157 (2006).

1. Introduction

Integrated optics that operate in the mid-infrared (mid-IR) region of the electromagnetic spectrum (3–25 μm) are attracting a considerable amount of research interest due to the potential applications in remote gas sensors [1], biosensors [2] and stellar interferometry [3]. Materials such as zinc selenide [4], silver halide [5], tellurium halides [6] and chalcogenide glasses [7] are suitable host materials for such devices due to their excellent mid-IR transparency.

Chalcogenide glasses are based on the chalcogen elements S, Se, and Te [8]. These glasses are formed by the addition of other elements such as Ge, As, Sb, Ga, etc. In addition to their transparency in the mid-IR they may also offer a high nonlinear refractive index (up to ~500 times that of fused silica), low-multi-photon absorption and high photosensitivity. Of the chalcogenide glasses, gallium lanthanum sulphide (GLS) is a particularly appealing candidate as it is thermally stable up to 550 °C, arsenic free and is commercially available.

Attempts to fabricate chalcogenide waveguides in the past have included fine embossing [9], liquid processing via capillary channel formation [10] and direct pulsed laser deposition [11], however these techniques involve several stages of heating and processing or give rise to high scattering losses. Here we have utilized the ultrafast laser inscription (ULI) technique [12] to fabricate single-mode waveguides embedded in a GLS substrate. We have used a femtosecond OPA and the z-scan technique to measure the magnitude of the nonlinear index of bulk GLS substrate and have then investigated the nonlinear properties of waveguides written into the material.

ULI is a powerful fabrication technique which relies on the nonlinear absorption of sub-bandgap photons to induce permanent structural changes to a material. These changes can manifest themselves in multiple ways including a change in refractive index [12] and/or an increased chemical etch rate [13]. Since ULI relies on a nonlinear absorption mechanism, the induced modification can be localized to the high intensity region at the focus of an ultra short pulse train. This gives ULI the unique advantage over other waveguide fabrication techniques of being capable of forming three dimensional structures [14]. ULI has been shown to be applicable to a multitude of materials including crystals [15] and amorphous

glasses [16]. ULI is a single step rapid fabrication technique that offers geometric as well as material design freedom. Using waveguide shaping techniques, mode sizes can be tailored for the particular application [17]. ULI has also been shown to be very suitable for inscribing fiber Bragg grating structures [18].

2. Waveguide fabrication

The waveguides were fabricated using a mode-locked Yb-doped fiber laser which emitted 300 fs pulses with a central wavelength of 1060 nm and a pulse repetition rate of 500 kHz. The pulse train from the laser was adjusted to be circularly polarized. The substrate was mounted on air bearing stages and pulses from the fabrication laser were focused inside the substrate to a distance of 240 μm from the top surface using a 50X (0.67 NA) aspheric lens. The single-scan writing technique was used. Fabrication pulse energies incident onto the sample were varied from 200 to 37 nJ in decreasing increments of 10%. Four different sample translation speeds were investigated: 0.2, 0.4, 0.6 and 0.8 mm s^{-1} with the substrate translation being perpendicular to the laser beam direction. After fabrication the input and output facets of the substrate were polished giving a sample length of 14.3 mm. The waveguide facets exhibit a distinct 'teardrop' shape similar to those observed in other chalcogenide glass substrates [19,20].

3. Waveguide characterization

Figure 1(a) shows the facet images for two waveguide structures which exhibited single-mode guiding at 2485 nm and 3850 nm respectively when viewed under a microscope in transmission mode. Waveguide I was inscribed with 113 nJ and a sample translation speed of 0.4 mm s^{-1} . Waveguide II was inscribed with 140 nJ pulses and a translation speed of 0.6 mm s^{-1} . Figure 1(b) shows the imaged end facets of the respective waveguides whilst coupling 2485 nm light into waveguide I and 3850 nm light into waveguide II – both guide a single transverse mode. The mode profiles were imaged over a distance of 34 cm with a ZnSe 20X (0.25 NA) aspheric lens and captured using a FLIR SC7000 camera. The $1/e^2$ mode field diameter for waveguide I for 2485 nm illumination was calculated to be 19.05 μm in the x-axis and 23.72 μm in the y-axis. The x- and y-axis mode field diameters for waveguide II under 3850 nm excitation were calculated to be 19.34 μm and 27.22 μm . The waveguide mode cross-sections are shown in Fig. 1(c).

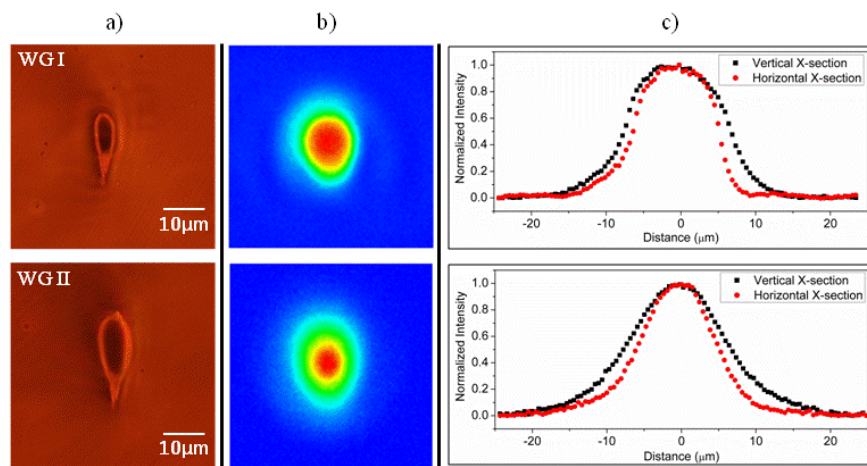


Fig. 1. (a) Facet images for waveguides I (upper) and II (lower) taken in transmission mode, (b) corresponding mode profile images [WG I guiding at 2485 nm. WG II guiding at 3850 nm.] and (c) their associated mode cross-sections in vertical and horizontal directions.

4. Nonlinear properties of GLS

The nonlinear guiding properties of waveguides I and II were investigated using a regeneratively amplified Ti: sapphire system operating at a pulse repetition rate of 1 kHz which then pumped an optical parametric amplifier (Newport Spectra-Physics OPA 800).

4.1 Measurement of bulk nonlinear refractive index at 2485 nm

In order to fully characterize the waveguides it is essential to study the nonlinear optical properties of the bulk material. To determine the magnitude and sign of the nonlinear refractive index of bulk GLS at 2485 nm a z-scan experiment [21] was performed on a 1 mm thick sample using the idler output of the OPA. The idler output was focused using a 200 mm focal length calcium fluoride lens and the sample translated through the focus along the beam path whilst recording the far field transmittance through an aperture using a PbSe amplified photodiode (Thorlabs PDA20H). Figure 2 shows a closed aperture z-scan trace with pulse energies of 500 nJ and an aperture transmission of 50%, the theoretical fit uses the simplified closed aperture fitting formula from [22]. The theoretical fit corresponds to a nonlinear refractive index of $7.8 \pm 0.9 \times 10^{-19} \text{ m}^2\text{W}^{-1}$ at 2485 nm.

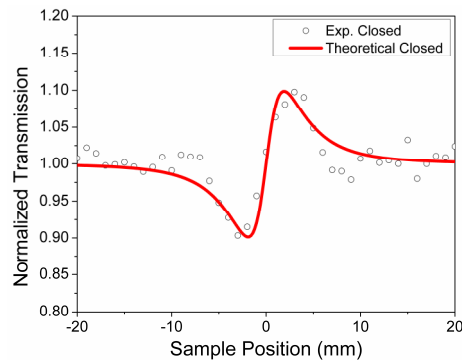


Fig. 2. Experimental closed aperture z-scan trace for GLS at 2485 nm. Theoretical (red line) fitted with $n_2 = 7.8 \times 10^{-19} \text{ m}^2\text{W}^{-1}$.

4.2 Transmission of femtosecond pulses in inscribed waveguides

The femtosecond pulse propagation properties of the inscribed waveguides were also investigated using the same laser system as outlined above. The idler output was tuned to investigate the nonlinear properties at 2485 nm. The OPA output was passed through an MgF_2 half-wave plate and a BaF_2 wire grid polarizer which were used for power and polarization control. Two 20X (0.25 NA) ZnSe aspheric lenses were used to couple and then collect the light from the test waveguide. This experimental arrangement is shown in Fig. 3. Incident power measurements were conducted using a pyro-electric detector (Laser Probe Inc. RkP-575) directly before the input coupling lens. After passing through a mechanical chopper the output was focused onto the entrance slit of a monochromator with a 5 cm focal length calcium fluoride lens. The monochromator (Zolix Omni λ -300) was used in conjunction with a PbSe detector and a lock-in amplifier in order to measure the spectral power distribution.

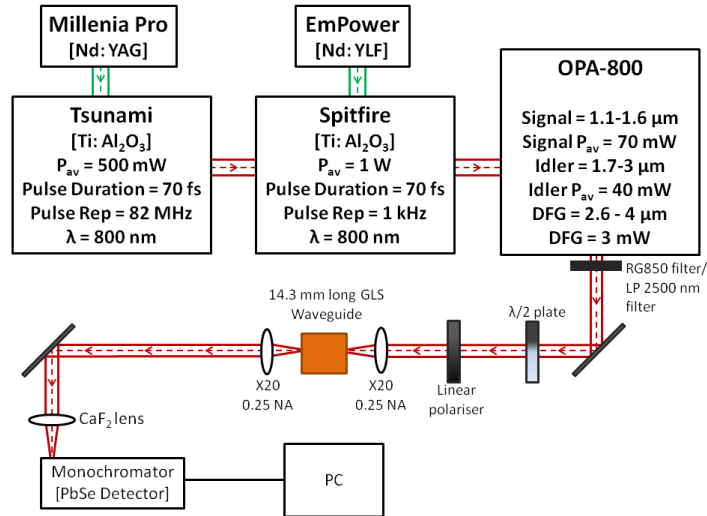


Fig. 3. Diagram of experimental set-up.

Figure 4(a) shows the transmitted spectrum of waveguide I when pulse energies of 72 and 130 nJ were incident onto the coupling lens. The input pump spectrum is also shown for comparison. Figures 4(b) and 4(c) show the individual broadened output spectra plotted with a linear scale with arrows indicating self-phase modulation peaks. The focusing spot diameter ($1/e^2$) of the input objective was measured to be 12.5 μ m. The minimum coupling loss was calculated to be 1.21 dB due to the spatial mis-match of the focused spot and that of the guided mode using the equation from [23]. The aspheric lens was measured to have a throughput loss of 0.97 dB, further losses due to Fresnel reflection at the waveguide facet would therefore yield maximum coupled pulse energies of 65.8 nJ (from 130 nJ incident) and 36.5 nJ (from 72 nJ incident).

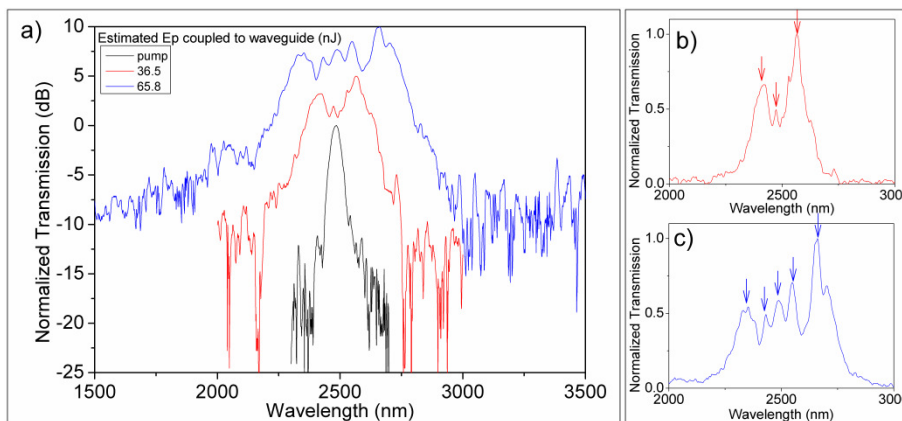


Fig. 4. (a) Graph showing normalized transmission spectra of waveguide I for incident femtosecond pulse energies of 72 and 130 nJ. For clarity, the graphs for the transmission spectra are each offset by 5 dB. (b) Linear scale normalized output of waveguide I with 72 nJ incident. (c) Linear scale normalized output of waveguide I with 130 nJ incident. Arrows indicate SPM peaks. Estimated coupled pulse energies were 36.5 and 65.8 nJ.

At the -15 dB points the broadened spectrum spanned 899 nm from 2002 nm to 2901 nm. The peak of the continuum with the most spectral power is red-shifted by 176 nm with respect to the input pulse wavelength and is evidence of stimulated Raman scattering.

A similar investigation was conducted using the difference frequency output of the OPA tuned to 3850 nm and coupled into waveguide II, a long-pass 2500 nm filter was placed in the beam path to block the residual signal and idler radiation. The wavelength of 3850 nm was selected as it is close to the material zero dispersion wavelength of the GLS substrate of 4000 nm. Figure 5 shows the span of continuum when 115 nJ pulses are incident onto the aspheric lens. At 3850 nm the aspheric lens was measured to give an input coupling spot size of $14.5 \mu\text{m}$, which would yield a 1.03 dB coupling loss to waveguide II. Taking into account the loss due to the spatial mis-match between the waveguide mode and the focusing spot, the Fresnel reflection loss and the loss incurred by the aspheric lens gave a maximum coupled pulse energy for propagation through the waveguide of 57 nJ (from 115 nJ incident). At the -15 dB points the continuum spanned 1588 nm from 2911 nm to 4499 nm from a 14.3 mm long waveguide.

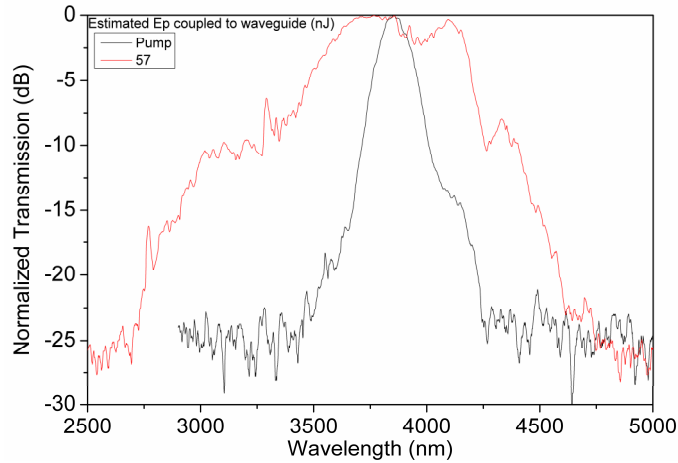


Fig. 5. Graph showing OPA pump input and spectrally broadened output after propagation through waveguide II with incident pulse energies of 115 nJ onto the coupling objective. Estimated coupled pulse energies were 57 nJ.

5. Discussion

We have demonstrated single-mode waveguide operation at two separate mid-IR wavelengths of 2485 nm and 3850 nm. Mode profiles showing slight ellipticity were recorded. The coupling losses due to mode mismatch were calculated to be in excess of 1 dB for both waveguides. Writing parameters can be optimized to give circularly symmetric mode profiles that can be coupled with low loss to, for example, single mode mid-infrared transmitting fibers.

The nonlinear refractive index of the bulk GLS substrate was measured using the z-scan technique at 2485 nm and its value was found to be $7.8 \pm 0.9 \times 10^{-19} \text{ m}^2\text{W}^{-1}$.

Since the pump wavelength is in the normal dispersion regime, the predominant mechanism for spectral broadening is self-phase modulation [24]. Figure 4 shows the onset of oscillations in the power spectral density with increasing pump power – which is a characteristic of self-phase modulation. The red shifting of the main spectral peak indicates that stimulated Raman scattering was another mechanism in the broadening of the femtosecond pulses. The broadened output spectrum of waveguide I showed five distinguishable peaks for coupled pulse energies of 65.8 nJ, this relates to a maximum nonlinear phase shift of 4.5π inside the waveguide [25] and for 36.5 nJ coupled pulse energy there are three SPM peaks resulting from a maximum phase change of 2.5π . The phase change, $\Delta\phi_{\text{NL}}$, due to nonlinear refractive index, n_2 , can be defined as: $\Delta\phi_{\text{NL}} = n_2 I k_0 L$, where $k_0 = 2\pi/\lambda$, I is the irradiance and L is the waveguide length. Using the maximum phase

change from the SPM peaks in Fig. 4 we can calculate a maximum n_2 for the modified region of $1.43 \times 10^{-19} \text{ m}^2\text{W}^{-1}$. This value is approximately 5 times lower than that measured using the z-scan technique. One factor that will lead to a discrepancy between the values of n_2 determined from the z-scan measurement and the SPM spectral inference is the dispersion occurring inside the waveguide; this will broaden the pulse width and reduce the effective irradiance along the sample length. Finally, it has been seen in studies on waveguides written inside fused silica substrates [26] that the ULI technique can cause changes to the nonlinear refractive index. It was shown that the waveguide nonlinear indices were up to four times lower than that of the unmodified regions and was very dependent on the writing parameters. It is planned to carry out z-scan measurements on large area modified GLS samples to examine its dependence on writing parameters, particularly writing speed. The continuum generated by waveguide II under 3850 nm pumping was smoother and a moderate blue shift with respect to the pump-wavelength was observed.

6. Conclusion

We have used the ULI technique to fabricate waveguides inside a GLS substrate. Two waveguides were characterized one of which supported single mode transmission at 2485 nm and the second supported single mode transmission at 3850 nm. Using waveguide shaping techniques the ellipticity of the waveguide mode can be reduced thereby reducing the coupling loss to circularly symmetric fiber modes. The nonlinear optical properties of these waveguides were studied using a femtosecond OPA. Nonlinear spectral broadening at pump wavelengths of 2485 nm and 3850 nm was investigated and both waveguides were found to spectrally broaden femtosecond pulses. At the -15 dB points the broadened radiation spanned 899 nm and 1588 nm respectively. Guided spectrally broadened radiation was recorded at wavelengths of greater than 4500 nm. This is the first report of guided radiation beyond $4 \mu\text{m}$ in an ULI fabricated waveguide. Continuum radiation guided in a single-mode at these wavelengths is of great interest for sensing applications and opens the way for truly integrated mid-IR optics. Analysis of the characteristic SPM peaks in waveguide I allowed an inference of the upper limit of the nonlinear refractive index of the modified GLS of $1.43 \times 10^{-19} \text{ m}^2\text{W}^{-1}$. We have also measured the nonlinear refractive index of the un-modified GLS substrate to be $7.8 \pm 0.9 \times 10^{-19} \text{ m}^2 \text{W}^{-1}$ using the z-scan method. The apparent reduction of nonlinear refractive index in unmodified material is large and efforts are underway to directly measure the nonlinear refractive index of modified GLS using z-scan of large modified regions, this will allow the investigation of the roles of various writing parameters on the change in nonlinear index, in particular variation of scan speed.

Acknowledgments

This work was funded by the UK Engineering and Physical Sciences Research Council (EPSRC EP/F067690/1 and EP/G030227/1). HTB is supported by a Royal Society of Edinburgh – Scottish Government Personal Research Fellowship. RRT acknowledges support through an STFC Advanced Fellowship (ST/H005595/1). This work is also partially funded by the ongoing Indo-UK collaboration under the UK-India Education and Research Initiative (UKIERI).